1

Background and System Model

In this first chapter, some basics regarding the propagation channel and the wireless transmission of an orthogonal frequency division multiplexing (OFDM) signal are recalled. Moreover, a brief state of the art of the pilot aided channel estimation methods is provided. Although the latter cannot be exhaustive, it covers some relevant techniques, in particular in an OFDM context.

1.1. Channel model

1.1.1. *The multipath channel*

The transmission channel (or propagation channel) is the environment situated between the transmitting and the receiving antennas. Whether an indoor or outdoor environment is considered, the signal transmitted over the channel suffers from some perturbations of different kinds: reflection, diffraction or diffusion. These phenomena are due to obstacles in the propagation environment, like buildings or walls. Besides, the transmitter, the receiver or both of them may be in motion, which induces Doppler effect.

In certain contexts, the transmitter and the receiver are in line of sight (LOS), so the channel is not destructive for the signal. On the contrary, in non-line of sight (NLOS) transmissions, the signal goes through several paths before reaching the receiving antenna. In that case, the propagation environment is called a multipath channel, and is mathematically written as a sum of weighted delayed Dirac impulses $\delta(\tau)$:

$$h(t,\tau) = \sum_{l=0}^{L-1} h_l(t)\delta(\tau - \tau_l), \tag{1.1}$$

where the channel impulse response (CIR) $h(t,\tau)$ depends on the number of paths L, the complex gains h_l and the delays τ_l. In this work, we will instead take an interest in NLOS transmissions. The channel frequency response (CFR) is obtained from [1.1] by means of the Fourier transform (FT) operation denoted by FT:

$$\begin{aligned} H &= FT_\tau(h) \\ H(t,f) &= \sum_{l=0}^{L-1} h_l(t)e^{-2j\pi f\tau_l}, \end{aligned} \tag{1.2}$$

where the subscript in $FT_{(.)}$ denote the variable on which the Fourier transform is processed. Figure 1.1 illustrates this relationship ((a): $h(t,\tau)$, and (b): $H(t,f)$). We can observe that the FT is made on the delay τ, which makes the frequency response $H(t,f)$ a time-varying function. When the channel does not vary, it is called static, and when the variations are very slow, the channel is called quasi-static. In this book, we will assume the latter scenario.

1.1.2. *Statistics of the channel*

1.1.2.1. *Rayleigh channel*

As numerous natural phenomena, the transmission channel is subject to random variations. Therefore, the instantaneous CIR [1.1] and CFR [1.2] are not sufficient to completely describe the channel. It becomes relevant to use the statistical characterization of the CIR and the CFR to study this random process.

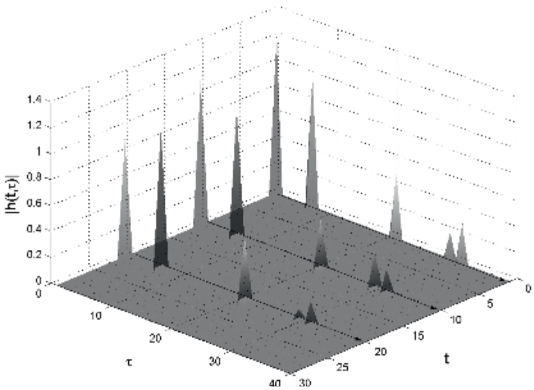

a) Impulse response $h(t, \tau)$

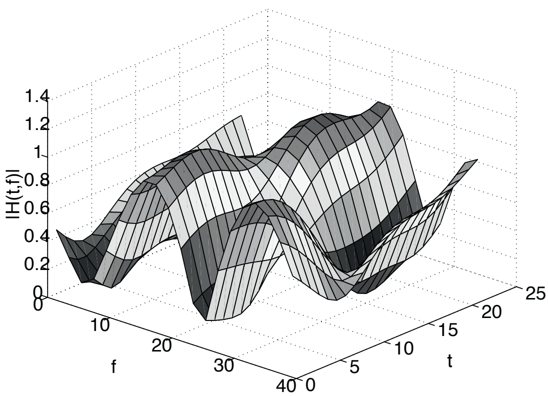

b) Frequency response $H(t, f)$

Figure 1.1. *Illustration of a time-varying impulse response* $h(t, \tau)$ *and a frequency response* $H(t, f)$ *of a multipath channel. For a color version of the figure, see www.iste.co.uk/savaux/mmse.zip*

In an NLOS transmission, due to the channel, the signal comes from all possible directions at the receiving antenna that is assumed to be isotropic. Thus, each delayed version of the received signal is considered as an infinite sum of random components. By applying the central limit theorem, $h(t)$ is then a zero-mean Gaussian complex process whose gain $|h(t)|$ follows a Rayleigh distribution [PAT 99] $p_{r,Ray}(r)$ of variance $\sigma_h^2 = E\{|h(t)|^2\}$:

$$p_{r,Ray}(r) = \frac{r}{\sigma_h^2} e^{\frac{-r^2}{2\sigma_h^2}}, \qquad [1.3]$$

where r is a positive real value. The probability density function (PDF) of the phase of a Rayleigh process follows a uniform distribution, noted $p_{\phi,Ray}(\theta)$:

$$\forall \theta \in [-\pi, \pi],\ p_{\phi,Ray}(\theta) = \frac{1}{2\pi}. \qquad [1.4]$$

The Rayleigh channel model is very frequently used, particularly in theoretical studies, since it is relatively close to reality, and the literature on Rayleigh distribution is very extensive. For these reasons, Rayleigh channels are considered all along this work. However, it does not cover all the possible scenarios: in a LOS context, the direct path adds a constant component to the previous model. In that case, $|h(t)|$ follows a Rice distribution, which is described in [RIC 48]. More recently, the Weibull model [WEI 51] has been proposed in order to describe real channel measurements with more accuracy. Nakagami model [NAK 60], later generalized in [YAC 00] by the $\kappa - \mu$ distribution, is also a global model from which Rayleigh's and Rice's are particular cases.

1.1.2.2. *WSSUS model*

The channel being a time-frequency varying random process, it is relevant to characterize it through its first and second-order statistic moments. According to Bello's work [BEL 63], let us assume a wide sense stationary uncorrelated scattering (WSSUS) model, defined as follows:

– WSS: each path $h_l(t)$ in [1.1] is a zero mean Gaussian complex process, i.e. $E\{h_l(t)\} = 0, \forall t$, with $E\{.\}$ the statistical expectation. Consequently, the mean of each path is independent from the time variations. Furthermore, the time correlation function $r_{h_l}(t_1, t_2) = E\{h_l(t_1)h_l^*(t_2)\}$ can be only written with the difference $\Delta_t = t_1 - t_2$, i.e.

$$r_{h_l}(t_1, t_2) = r_{h_l}(\Delta_t). \quad [1.5]$$

Each path $h_l(t)$ of the channel is then wide sense stationary.

– US: the paths are uncorrelated, so for $l_1 \neq l_2$, we have

$$E\{h_{l_1}(t)h_{l_2}^*(t)\} = 0. \quad [1.6]$$

This model is used in the following to apply the proposed detection and channel estimation algorithm. However, it does not necessarily match the reality, so we will also study the performance of the proposed method under channel model mismatch, particularly in Chapter 3.

Let us also define two very useful statistical functions that characterize the channel along the delay and the frequency axes:

– The intensity profile $\Gamma(\tau)$. A commonly used model is the decreasing exponential [EDF 98, STE 99, FOE 01].

– The frequency correlation function of the channel $R_H(\Delta_f)$, whose expression will be detailed later.

These two functions are linked by Fourier transform:

$$\begin{aligned} &\Gamma = FT^{-1}_{\Delta_f}(R_H) \\ \Leftrightarrow\ &R_H = FT_\tau(\Gamma). \end{aligned} \quad [1.7]$$

Figure 1.2 depicts the decreasing intensity profile and the real and imaginary parts of the frequency correlation function.

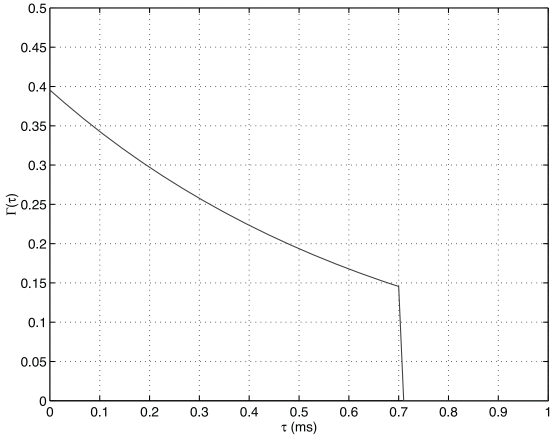

a) Channel Intensity profile $\Gamma(\tau)$.

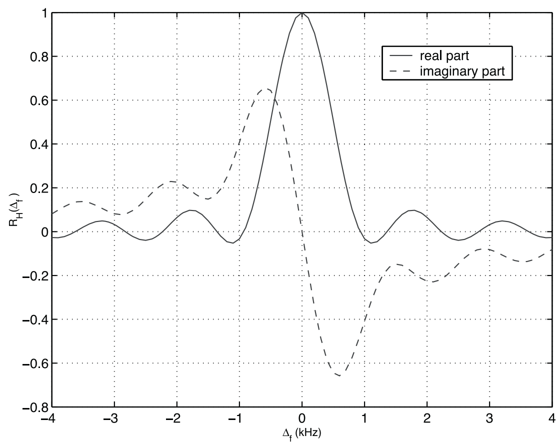

b) Frequency Correlation Function $R_H(\Delta_f)$.

Figure 1.2. *Link between the channel intensity profile and the frequency correlation function*

1.2. Transmission of an OFDM signal

When combined with a channel coding, the transmission of data using a frequency multiplexing is very robust against the frequency selective channels, in comparison with single-carrier modulations [SCO 99, DEB]. The use of orthogonal subcarriers has been proposed since the 1950s, in particular for military applications, but the acronym OFDM appeared in the 1980s, when the evolution of the technology of semiconductors enabled a great development of the implementation of complex algorithms, especially the algorithms based on large size FFT/IFFT. This kind of modulation is now used in a large number of wired and wireless transmission standards.

1.2.1. *Continuous representation*

In the continuous formalism, the baseband OFDM signal is written as:

$$s(t) = \sum_{n \in \mathbb{Z}} s_n(t) = \sqrt{\frac{1}{T_s}} \sum_{n \in \mathbb{Z}} \sum_{m=0}^{M-1} C_{m,n} \Pi(t - nT_s) e^{2j\pi m F_s t}, \qquad [1.8]$$

where $s_n(t)$ is the n^{th} OFDM symbol, $\Pi(t)$ is the rectangular function of duration T_s as

$$\Pi(t) = \begin{cases} 1 & \text{if } -\frac{T_s}{2} \leq t < \frac{T_s}{2} \\ 0 & \text{else,} \end{cases} \qquad [1.9]$$

where $F_s = \frac{1}{T_s}$ is the subcarrier spacing, M is the number of subcarriers such as, if we denote by B the bandwidth, we have $F_s = B/M$. The scalar $C_{m,n}$ with $m = 0, 1, ..., M-1$ are the information symbols coming from a set Ω of a given constellation, such as the binary phase shift keying (BPSK) or the four-quadrature amplitude modulation (4-QAM). The different subcarriers of the OFDM symbols are orthogonally arranged, thus, no interference occurs in the frequency domain (see Figure 1.3). The received signal $u(t)$ is the convolution of $s(t)$ and $h(t)$, plus the white Gaussian noise denoted by $w(t)$. In the frequency domain, due to the Fourier transform property, the convolution becomes a simple product:

$$u(t) = (h \star s)(t) + w(t) \quad [1.10]$$

$$\stackrel{FT}{\Longrightarrow} U(f) = H(f).C(f) + W(f). \quad [1.11]$$

So as to cancel the intersymbol interferences (ISIs) due to the delayed paths of the channel, the solution consists of adding a guard interval (GI) at the head of each OFDM symbol. If the GI length is greater than the maximum delay of the channel, it contains all the interferences from the previous symbol, and the GI removal cancels the ISI. In the following, let us assume that the GI is a cyclic prefix, i.e. the end of each OFDM symbol is copied at its head. As noted later, in addition to the ISI cancellation, the use of a CP gives a cyclic structure to the OFDM symbols. Let us denote by T_{CP} the duration of the CP.

Figure 1.3 shows the effects of the channel on the OFDM signal in the time and the frequency domains. Figure 1.3(a) illustrates, in the time domain, the ISI cancellation due to the CP removal. The frequency orthogonality is displayed in Figure 1.3(b). The robustness of the OFDM against the multipath channel lies in the fact that, by considering a sufficiently small intercarrier spacing F_s, one can assume that the channel is flat on each subcarrier. Consequently, a simple division per subcarrier is processed to recover the data that has been transmitted. As a matter of fact, this property is ensured when the receiver is perfectly synchronized with the signal. That will be assumed in most of the further developments. However, we will study the effect of a synchronization mismatch on the performance of the proposed detector.

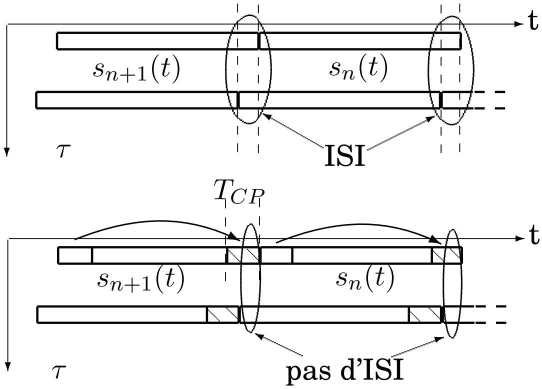

a) ISI cancellation thanks to the cyclic prefix.

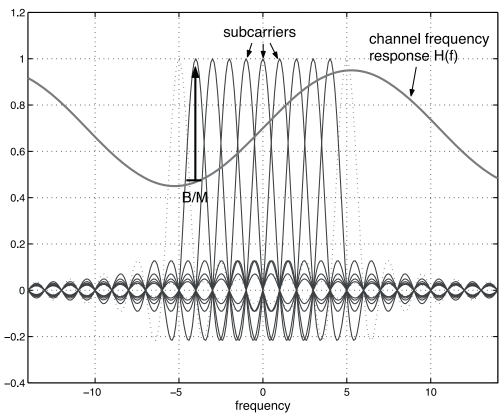

b) Frequency orthogonality between subcarriers, and effect of the channel frequency response.

Figure 1.3. *Time and frequency properties of the OFDM with cyclic prefix. For a color version of the figure, see www.iste.co.uk/savaux/mmse.zip*

1.2.2. *Discrete representation*

The orthogonal parallel subcarriers of the OFDM signal naturally leads to a discrete representation of the signal. Moreover, we perform a digital signal processing, and the discrete version of the FT, called discrete Fourier transform

(DFT), allows a generation of the OFDM symbols with a low computation cost. Note that, when the DFT size is a power of two, a fast Fourier transform (FFT) algorithm can be performed. In the discrete formalism, the use of the CP transforms the linear convolution [1.11] into a cyclic convolution [PEL 80] and, after the CP removal, the n^{th} received OFDM symbol is then given by

$$\mathbf{u}_n = \begin{pmatrix} h_{0,n} & 0 & \cdots & \cdots & h_{L-1,n} & \cdots & h_{1,n} \\ h_{1,n} & h_{0,n} & 0 & \ddots & \ddots & \ddots & \vdots \\ \vdots & \ddots & \ddots & & \ddots & \ddots & h_{L-1,n} \\ h_{L-1,n} & \ddots & \ddots & h_{0,n} & 0 & \ddots & 0 \\ 0 & \ddots & \ddots & & \ddots & \ddots & \vdots \\ \vdots & \ddots & \ddots & & \ddots & \ddots & 0 \\ 0 & \cdots & 0 & h_{L-1,n} & \cdots & h_{1,n} & h_{0,n} \end{pmatrix} \begin{pmatrix} s_{0,n} \\ s_{1,n} \\ \vdots \\ \vdots \\ s_{M-1,n} \end{pmatrix} + \mathbf{w}_n$$

$$= \underline{\mathbf{h}}_n \mathbf{s}_n + \mathbf{w}_n, \qquad [1.12]$$

where $\underline{\mathbf{h}}_n$ is the $M \times M$ circulant matrix of the channel, $\mathbf{s}_n$ is the $M \times 1$ vector containing the samples of the symbol $s_n(t)$, and $\mathbf{w}_n$ is the noise vector of size $M \times 1$. The circulant matrices are diagonalizable in the Fourier basis (see [GRA 06, CON]), whose matrix $\underline{\mathcal{F}}$ is given by

$$\underline{\mathcal{F}} = \frac{1}{\sqrt{M}} \begin{pmatrix} 1 & 1 & 1 & \cdots & 1 \\ 1 & \omega & \omega^2 & \cdots & \omega^{(M-1)} \\ 1 & \omega^2 & \omega^4 & \cdots & \omega^{2(M-1)} \\ \vdots & \vdots & \vdots & \ddots & \vdots \\ 1 & \omega^{(M-1)} & \omega^{2(M-1)} & \cdots & \omega^{(M-1)^2} \end{pmatrix}, \qquad [1.13]$$

with $\omega = e^{-\frac{2j\pi}{M}}$. It can be noticed that $\underline{\mathcal{F}}$ is an orthonormal matrix, i.e. $\underline{\mathcal{F}}\underline{\mathcal{F}}^H = \underline{\mathbf{I}}$, where $\underline{\mathbf{I}}$ is the identity matrix and ^{H} is the Hermitian transpose (or conjugate transpose). To get the frequency samples of the received signal, we calculate the

DFT of $\mathbf{u}_n$ by $\mathbf{U}_n = \underline{\mathcal{F}}\mathbf{u}_n$. The matrix $\underline{\mathbf{h}}_n$ being diagonal in the Fourier basis, we simplify to get:

$$\begin{aligned}\mathbf{U}_n &= \underline{\mathcal{F}}\underline{\mathbf{h}}_n\underline{\mathcal{F}}^H\underline{\mathcal{F}}\mathbf{s}_n + \mathbf{W}_n \\ &= \underline{\mathcal{F}}\underline{\mathbf{h}}_n\underline{\mathcal{F}}^H\mathbf{C}_n + \mathbf{W}_n \\ &= \underline{\mathbf{H}_n}\mathbf{C}_n + \mathbf{W}_n,\end{aligned} \quad [1.14]$$

where $\mathbf{C}_n = \underline{\mathcal{F}}\mathbf{s}_n$ is the $M \times 1$ vector containing the data $C_{m,n}$. The diagonal matrix $\underline{\mathbf{H}_n}$ is composed of the samples $H_{m,n}$ of the frequency response that is the DFT of the CIR:

$$\begin{aligned}H_{m,n} &= \sum_{l=0}^{L-1} h_{l,n} e^{-2j\pi f_m \beta_l \tau_s} \\ &= \sum_{l=0}^{L-1} h_{l,n} e^{-2j\pi \frac{m}{M}\beta_l},\end{aligned} \quad [1.15]$$

where $f_m = \frac{m}{M\tau_s}$ and $\beta_l = \frac{\tau_l}{\tau_s}$ sampled versions of f and τ_l, with τ_s the sampling time. Since $\underline{\mathbf{H}_n}$ is a diagonal matrix, it is usual to find an equivalent expression to [1.14]:

$$\begin{aligned}&\mathbf{U}_n = \underline{\mathbf{H}}_n\mathbf{C}_n + \mathbf{W}_n \\ \Leftrightarrow\ &\mathbf{U}_n = \underline{\mathbf{C}}_n\mathbf{H}_n + \mathbf{W}_n,\end{aligned} \quad [1.16]$$

where $\underline{\mathbf{C}}_n$ is the diagonal matrix containing the samples of the vector $\mathbf{C}_n$. Moreover, each sample of $\mathbf{U}_n$ can be written as a simple scalar factor

$$U_{m,n} = H_{m,n}C_{m,n} + W_{m,n}. \quad [1.17]$$

This shows that if the CP is well sized, it fully cancels the ISI and each transmitted symbol $C_{m,n}$ is only corrupted by the channel frequency coefficient $H_{m,n}$ and the noise $W_{m,n}$. This expression is widely exploited for the channel estimation, which will be discussed further in this work.

1.2.3. *Discrete representation under synchronization mismatch*

In [1.14], the receiver is supposed to be synchronized with the transmitted signal. In practice, the observation window of the receiver may not match the OFDM symbol, as illustrated in Figure 1.4. We then define δ the time shift. In that case, we rewrite the transmission equation [1.14] by taking into account the interference $\mathbf{I}(\delta)$ induced by δ:

$$\mathbf{U}_n = \underline{\mathbf{H}_n}\mathbf{C}_n + \mathbf{I}(\delta) + \mathbf{W}_n, \qquad [1.18]$$

where $\mathbf{I}(\delta)$ is the sum of an intercarrier interference term $\mathbf{I}^c(\delta)$ and an ISI term $\mathbf{I}^s(\delta)$. The former is due to the loss of the cyclic property implying a loss of orthogonality between the subcarriers; the latter is due to the several samples coming from the adjacent OFDM symbols.

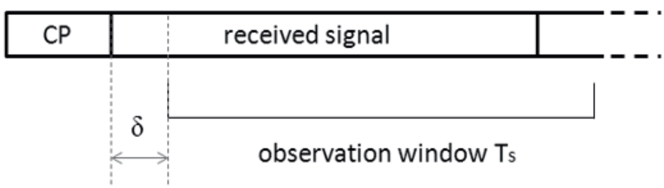

Figure 1.4. *Synchronization mismatch δ between the received signal and the observation window*

Although the receiver will be considered to be perfectly synchronized with the signal in Chapter 2, the synchronization mismatch will be taken into account to characterize the detector performance in Chapter 3.

1.3. Pilot symbol aided channel and noise estimation

1.3.1. *The pilot arrangements*

Among the wide range of channel and noise estimation techniques, we here focus on the one called "pilot symbol aided method" (PSAM) or "data aided estimation" (DAE). The pilots are particular subcarriers whose gain, phase and arrangement in the OFDM frame are known from the transmitter and the receiver. The pilot pattern depends on the time and frequency selectivity of the channel. As recalled in [OZD 07], in order to capture all the variations of the channel, the pilot gaps over the frequency axis D_p and the time axis D_t must respect the Nyquist sampling theorem:

$$D_p \leq \frac{1}{\tau_{L-1} F_s}, \qquad [1.19]$$

and

$$D_t \leq \frac{1}{2 f_{D,max} T_s}, \qquad [1.20]$$

where $f_{D,max}$ is the maximum Doppler frequency. Figure 1.5 shows two usually considered arrangements in theoretical studies: (a) the block-type arrangement (also called preamble) and (b) the comb-type arrangement. The first arrangement is adapted to quasi-static channels with high-frequency selectivity. On the contrary, the comb-type arrangement (2) is used when the channel is time selective and with a low-frequency selectivity. Since we consider quasi-static channel, we will use the block-type pilot pattern.

In practical applications, such as in digital TV transmission with the digital video broadcasting-terrestrial (DVB-T) [ETS 04] standard, digital radio with the digital radio mondiale (DRM) [ETS 09] standard, or Wi-Fi [IEE 07], scattered pilots are rather considered. In that case, less subcarriers are dedicated to the channel estimation, which improves the data rate compared to the patterns of Figure 1.5, with almost the same performance.

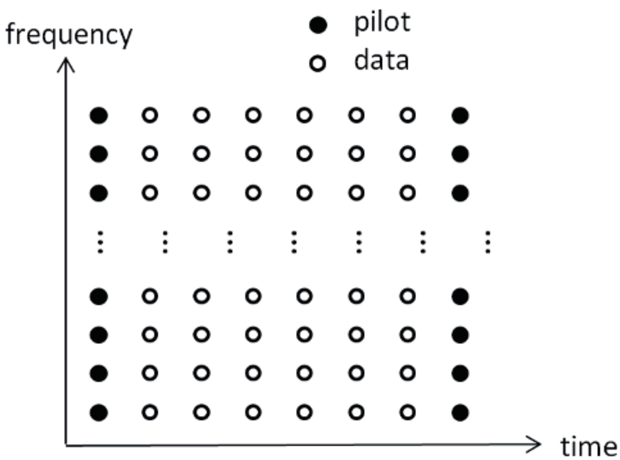

a) Block-type arrangement

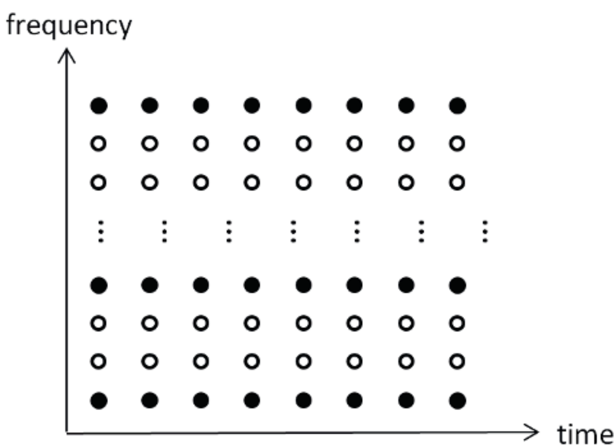

b) Comb-type arrangement

Figure 1.5. *Two possible pilot arrangements in the OFDM frame*

Whatever the pattern, we can see in Figure 1.5 that if the channel is known on the pilot tones' position, an interpolation is required to estimate the channel on all the positions of the time and frequency lattice. Some of channel estimation techniques are presented below.

1.3.2. *Channel estimation*

In the following, the developments are performed on a preamble scheme, although the results remain valid if the tones are sparsely distributed in the OFDM frame. First we detail the least square (LS) and the linear minimum mean square error (LMMSE) methods, because they are the most used and studied, and the technique proposed in this work is based on LMMSE. Second, we cover some of usual other techniques. For a clarity purpose, the subscript n is removed in the further equations.

1.3.2.1. *LS estimation*

The LS criterion aims to minimize the cost function J_{LS} that is defined as the square absolute value of the difference between the vector of the received signal $\mathbf{U}$ and the product of the transmitted signal vector $\mathbf{C}$ by a diagonal matrix $\underline{\mathbf{D}}$ whose coefficients have to be optimized. Then we get the estimation $\hat{\mathbf{H}}^{LS} = \underline{\mathbf{D}}_{opt}$. The cost function is first expressed as

$$J_{LS} = |\mathbf{U} - \underline{\mathbf{D}}\mathbf{C}|^2. \qquad [1.21]$$

Let us define the optimal matrix $\underline{\mathbf{D}}_{opt} = \hat{\underline{\mathbf{H}}}^{LS}$, where $\hat{\underline{\mathbf{H}}}^{LS}$ is the LS estimation of the CFR. After some mathematical developments, minimizing J_{LS} leads to

$$\hat{H}_m^{LS} = \frac{U_m}{C_m} = H_m + \frac{W_m}{C_m}, \qquad [1.22]$$

namely, in a matrix form:

$$\hat{\mathbf{H}}^{LS} = \mathbf{U}\underline{\mathbf{C}}^{-1} = \mathbf{H} + \mathbf{W}\underline{\mathbf{C}}^{-1}. \quad [1.23]$$

From [1.23], it can be seen that the LS estimation is very sensitive to the noise level. To reduce the sensitivity to the noise, [BIG 04] proposes the scaled LS (SLS) estimator, in which $\hat{\mathbf{H}}^{LS}$ is multiplied by a coefficient γ, which is chosen such as the mean square error $E\{||\mathbf{H} - \gamma\hat{\mathbf{H}}^{LS}||_F^2\}$ is minimized, with $||.||_F$ the Frobenius norm[1]

1.3.2.2. *LMMSE estimation*

The LMMSE aims to minimize the cost function defined by the mean square error of the error vector $\mathbf{H} - \underline{\mathbf{D}}\mathbf{U}$, as shown in [KAY 03b]:

$$J_{LMMSE} = E\{||\mathbf{H} - \underline{\mathbf{D}}\mathbf{U}||_F^2\}, \quad [1.24]$$

where $\underline{\mathbf{D}}$ is the matrix whose coefficients have to be optimized. The LMMSE channel estimation is then given by $\hat{\mathbf{H}}^{LMMSE} = \underline{\mathbf{D}}_{opt}\mathbf{U}$. The development of [1.24] yields:

$$\begin{aligned} \hat{\mathbf{H}}^{LMMSE} &= \underline{\mathbf{D}}_{opt}\mathbf{U} \\ &= \underline{\mathbf{R}}_H(\underline{\mathbf{R}}_H + (\underline{\mathbf{C}}\underline{\mathbf{C}}^H)^{-1}\sigma^2\underline{\mathbf{I}})^{-1}\underline{\mathbf{C}}^{-1}\mathbf{U} \\ &= \underline{\mathbf{R}}_H(\underline{\mathbf{R}}_H + (\underline{\mathbf{C}}\underline{\mathbf{C}}^H)^{-1}\sigma^2\underline{\mathbf{I}})^{-1}\hat{\mathbf{H}}^{LS}, \end{aligned} \quad [1.25]$$

where $\underline{\mathbf{R}}_H = E\{\mathbf{H}\mathbf{H}^H\}$ is the channel covariance matrix. LMMSE is, by definition, the optimal estimator in the sense of the mean square error. However, we notice in [1.25] that LMMSE has two main drawbacks: first, LMMSE is far more complex than LS, due to the matrix inversion and

1 The matrix Frobenius norm of a matrix $\underline{\mathbf{A}}$ is defined by $||\underline{\mathbf{A}}||_F = \sqrt{tr(\underline{\mathbf{A}}\underline{\mathbf{A}}^H)}$.

multiplication. Second, LMMSE requires the second-order moments of the channel $\underline{\mathbf{R}}_H$ and of the noise σ^2, which are *a priori* unknown. The algorithm detailed in this book has been originally proposed to address this latter drawback, by iteratively estimating the noise level and the channel by means of the MMSE criterion.

1.3.2.3. *Other estimation techniques*

Due to the LS estimator, the noisy CFR is obtained on the pilot tones. In numerous cases, an interpolation is then required to estimate the channel on the whole subcarriers of the time and frequency lattice. A very wide range of estimation methods is described in the literature, so it is impossible to draw up an exhaustive list, but around 20 of the most used techniques are described in [HSI 98, JAF 00, MOR 01, COL 02, SHE 06, DON 07]. Among them, we will cite the 2D Wiener filter, described in [HOE 97], which is the generalized form of the optimal LMMSE estimator over the two-dimensions time and frequency. However, its practical implementation is limited by its very high computation cost. Far more simple, the interpolated fast Fourier transform (iFFT) (do not mistake for inverse FFT) [SCH 92, LE 07] is a very usual interpolation method in signal processing. After having performed the LS estimation on the pilot subcarriers, the estimated CIR is computed by means of an IFFT. Then, some zeros are added at the end of the estimated IR vector (zero padding) and finally, an FFT is done to get the estimated CFR. As mentioned in [SCH 92], the iFFT channel estimation suffers from the leakage that is induced in the adjacent channel. Another usual estimator, called maximum likelihood (ML) and described in [KAY 03a, ABU 08], aims to minimize the cost function J_{ML}:

$$J_{ML} = \ln(p(\mathbf{U}_n|\mathbf{H}_n, \underline{\mathbf{C}}_n, \sigma^2)), \qquad [1.26]$$

where $p(\mathbf{U}_n|\mathbf{H}_n, \underline{\mathbf{C}}_n, \sigma^2)$ is the conditional PDF of the received signal. As indicated in [WIE 06], in the case of a preamble, maximizing J_{ML} is exactly equivalent to minimizing J_{LS} in [1.21]. ML becomes very useful when the number of pilots is lower than the FFT size, even though, in that case, the maximization of J_{ML} has a very high calculation cost. To reduce this complexity, the expectation-maximization (EM) algorithm was originally proposed in 1977 by Dempster *et al.* in [DEM 77]. This is an iterative algorithm whose performance tends to that of the MLs when the iterations number increases.

Some interpolation methods based on polynomials are also commonly used in practical implementations. Indeed, they are more simple than the previous methods, and do not require any knowledge of the channel or signal statistics. In particular, we can cite:

– The nearest-neighbor (NN) interpolation is the most simple as it uses a polynomial of degree zero. Thus, for a given frequency position f near a pilot position f_p, the NN interpolator is expressed by:

$$\hat{H}(f) = \hat{H}(f_p). \qquad [1.27]$$

Despite its simplicity, it is obvious that this method is only adapted for channel that are very weakly selective.

– The linear interpolation uses polynomials of degree one. Thus, for a value $f \in [f_p, f_{p+\delta_f}]$, where δ_f is the gap between two consecutive pilots, the estimated channel $\hat{H}(f)$ is expressed by

$$\hat{H}(f) = \hat{H}(f_p) + (f - f_p)\frac{\hat{H}(f_{p+\delta_f}) - \hat{H}(f_p)}{f_{p+\delta_f} - f_p}. \qquad [1.28]$$

In the same way as the NN interpolation, this method is not accurate when the channel is highly frequency selective.

– The polynomial interpolation consists of approximating the channel $H(f)$ by a polynomial of degree $P-1$, with P the number of pilot tones in an OFDM symbol. If a Lagrange polynomial basis $\{\mathcal{L}_0, \mathcal{L}_1, ..., \mathcal{L}_{P-1}\}$ is used, the interpolated channel is written as:

$$\hat{H}(f) = \sum_{p=0}^{P-1} \mathcal{L}_p(f)\hat{H}(f_p). \quad [1.29]$$

The polynomial interpolation with Lagrange basis is limited by the Runge effect that results in a divergence of the estimated values between the nodes f_p when P increases. A solution consists of splitting the whole interval into several consecutive intervals containing four nodes. An interpolation of degree three is then applied in each subinterval. This solution, called piecewise cubic interpolation, is widely used. However, the interpolated channel considering the whole bandwidth B is not continuous, since cubic polynomials are concatenated. To get a continuous function, it is possible to perform the interpolation method called spline. This technique, using a Hermite polynomial basis, imposes a condition on the first derivative of the interpolated function that makes it continuous on each node.

1.3.3. *Noise variance estimation*

In addition to the multipath channel, the noise is one of the main source of disturbance for the transmitted signal. The noise is often characterized either by its power (or variance), or by the signal-to-noise ratio (SNR), i.e. by comparison with the signal level. This measurement can then be used for the design of the transmitter and the receiver. For instance, at the transmitter side, the constellation type and its size can be updated according to the SNR level [KEL 00]. At the receiver side, many algorithms such as the turbo-decoder [SUM 98] or the LMMSE channel estimation (see [1.25], [VAN 95]) require the knowledge of the SNR. We are particularly interested by the latter application in this work, since the estimator in Chapter 2 iteratively estimates the channel and the noise variance by means of the MMSE criterion.

The SNR estimation methods are commonly based on three elementary steps:

1) The noise variance estimation $\hat{\sigma}^2$ is first performed.

2) An estimation of the transmitted signal power $\hat{P}_s$ is achieved.

3) The SNR, noted ρ is finally obtained by $\hat{\rho} = \hat{P}_s/\hat{\sigma}^2$.

Alternatively, the steps (2) and (3) are sometimes replaced by the following processing:

2) The second-order moment of the received signal is estimated by $\hat{M}_2 = \hat{P}_s + \hat{\sigma}^2$.

3) the SNR is estimated by $\hat{\rho} = \hat{M}_2/\hat{\sigma}^2 - 1$.

The main difference between the techniques of the literature lies in the way to estimate σ^2. A wide range of usual methods are described in [PAU 00, LI 02, REN 05]. Among them, the second- and fourth-order moment (M_2M_4) estimator is first mentioned in [BEN 67]. Its principle is to estimate the second-order moment of the received signal U_m as $M_2 = E\{U_m U_m^*\} = P_s + \sigma^2$ on the one hand, and the fourth-order moment $M_4 = E\{(U_m U_m^*)^2\} = P_s^2 + 4P_s\sigma^2 + 2\sigma^4$ on the other hand. Then, the signal and the noise powers estimations are deduced by:

$$\hat{P}_s = \sqrt{2\hat{M}_2^2 - \hat{M}_4} \qquad [1.30]$$

$$\hat{\sigma}^2 = \hat{M}_2 - \sqrt{2\hat{M}_2^2 - \hat{M}_4}. \qquad [1.31]$$

In [REN 05], an alternative M_2M_4 method is proposed, using a new definition of the fourth order moment $M_4' = E\{(\mathfrak{Re}(U_m)^2 + \mathfrak{Im}(U_m)^2)^2\}$, where $\mathfrak{Re}(.)$ and $\mathfrak{Im}(.)$

denote the real part and the imaginary part of a complex number, respectively. The advantages of the M_2M_4 lie in the facts that it does not require any channel estimation and that it has a low complexity. However, its efficiency is degraded if the channel is frequency selective.

The ML estimator, whose developments are given in [KAY 03b] for the noise variance estimation, supposes the channel to be known, or requires a high complexity, as previously mentioned. The minimum mean square error (MMSE) estimator

$$\hat{\sigma}^2 = \frac{1}{M} E\{||\mathbf{U} - \mathbf{CH}||_F^2\}, \quad [1.32]$$

from which the method that is proposed in this work is derived, also requires the CFR, which is practically replaced by its estimated value. Thus, the performance of the MMSE estimation depends on the channel estimation. References such as [PAU 00, BOU 03, XU 05a] only derive a theoretical expression of the MMSE in which the channel is supposed to be known, but the authors do not propose any practical solution to reach it.

These usual methods can be derived in the OFDM context, as it is done by the authors of [XU 05a]. If, in addition, a frequency selective channel is considered, the literature proposes two strategies for the SNR estimation. The first strategy uses the previously cited methods, and requires a channel estimation. In the second strategy, the estimation of the CFR is avoided [BOU 03, REN 09]. In [BOU 03], the author proposes a method for a 2×2 multi input multi output (MIMO) configuration that features a two pilot-symbols preamble and assumes that the channel coefficients are invariant over two consecutive carriers. Following a similar scheme, [REN 09] also proposes a preamble-based method using two pilot symbols for the the noise variance estimation. The received symbols in the preamble are then expressed by

$\mathbf{U}_n = \underline{\mathbf{C}}_n\mathbf{H}_n + \mathbf{W}_n$ and $\mathbf{U}_{n+1} = \underline{\mathbf{C}}_{n+1}\mathbf{H}_{n+1} + \mathbf{W}_{=1}$, where $\underline{\mathbf{C}}_{n+1}\mathbf{H}_{n+1}$ is supposed to be equal to $\underline{\mathbf{C}}_n\mathbf{H}_n$. Thus, the channel estimation is avoided because the noise variance is simply estimated by:

$$\hat{\sigma}^2 = \frac{1}{2}E\{||\mathbf{U}_n - \mathbf{U}_{n+1}||^2\}. \qquad [1.33]$$

Although it is an efficient method, its main drawback is the loss of data rate due to the need of a preamble composed of two pilots. This is especially the case if a preamble must be regularly inserted, as in the case of time-varying channels. In [XU 05b], the SNR is estimated by means of the properties of the channel covariance matrix. As presented in section 1.1, the channel has a length L. Thus, its covariance matrix has L non-null eigenvalues from which M_2 is estimated and $M - L$ null eigenvalues from which σ^2 is estimated. This method is limited by the channel insufficient statistics, which degrades the estimation performance.

1.4. Work motivations

This work focuses on the MMSE-based channel and noise variance estimation. As has been mentioned, LMMSE is the optimal channel estimator in the sense of the mean square error, but it requires the second-order moments of the channel and the noise to be performed (see [1.25]). However, these parameters are usually unknown at the receiver and must be estimated. The solution detailed in this work consists of feeding the LMMSE estimation by the optimal MMSE estimated noise level [1.32]. To best match the unknown CFR, we propose to replace it by its LMMSE estimated value, so it clearly appears that one estimation feeds the other estimation. As a result, it seems natural to propose an iterative algorithm for the joint estimation of the noise variance and the channel. Since we suppose no *a priori* CSI at the receiver, this algorithm is valid for communications systems such as Wi-Fi or LTE, and for broadcast systems such as DRM/DRM+ [ETS 09] or DVB-T [ETS 04] as well.

In addition to the joint noise and channel estimation, it is possible to use the proposed estimator to measure the noise level in a free band, by keeping exactly the same structure. Thus, according to a given detection test, the algorithm enables the receiver to determine if a user is in a band or not. The two different uses of the technique, estimator and detector are described in Chapters 2 and 3, respectively.